Optimisation of Performance Rowing Blades

Journal:	*Part P: Journal of Sports Engineering and Technology*
Manuscript ID	JSET-25-0301.R2
Manuscript Type:	Original Research Article
Date Submitted by the Author:	22-Apr-2026

Complete List of Authors:	Morgan, Ben; Swansea University Faculty of Science and Engineering, Mechanical Engineering Morgan, Ben ; Swansea University Faculty of Science and Engineering Harrison, Will; Swansea University Faculty of Science and Engineering

Keywords:	Oar, Drive Phase, Fluid Forces, Lateral Velocity, Max Force Angle, Power Curve, Gearing, Computational Fluid Dynamics, Concept2, Rowing

Abstract:	Rowing blades (oars) transfer power from athletes to the water to propel a boat forward. The complex nature of fluid forces around a blade has only recently started to be understood with previous studies only investigating blades that are commercially available. The full motion of a blade spoon through water is complex, with motion both longitudinal and perpendicular to the boat motion. This multidisciplinary research uses a combination of computational models with experimental analysis to evaluate how spoon shapes affect the fluid forces on a blade during rowing. The computational model used 3D computational fluid dynamics (CFD) to evaluate the drag and lift forces around four different spoon shapes as they rotate through moving water. Each design had the same surface area, with different positions of maximum depth along their length. Experimental analyses used telemetry to measure blade forces during a series of rowing runs, for two different Concept2 blades, over different stroke rates and blade gearing. The results showed there was a correlation of R^2=0.78 between the location of the spoon's maximum depth and the lift force generated at the catch. The study also found that, a resultant fluid force change of 47.3 N, at the spoon, can promote a -10.7° ± 1.7° shift in the maximum force angle in the real world. The shift in maximum force angle highlighted how spoon design, especially regarding position of the maximum depth, affected the profile of the rowing stroke.

Optimisation of Performance Rowing Blades

Ben I Morgan, Ben W Morgan, Will J Harrison
Department of Mechanical Engineering, Swansea University, Fabian Way, Swansea, SA1 8EN
Corresponding author: Ben I Morgan

ben@mc-solutions.uk, W.Harrison@Swansea.ac.uk

Abstract

Rowing blades (oars) transfer power from athletes to the water to propel a boat forward. The complex nature of fluid forces around a blade has only recently started to be understood with previous studies only investigating blades that are commercially available. The full motion of a blade spoon through water is complex, with motion both longitudinal and perpendicular to the boat motion. This multidisciplinary research uses a combination of computational models with experimental analysis to evaluate how spoon shapes affect the fluid forces on a blade during rowing. The computational model used 3D computational fluid dynamics (CFD) to evaluate the drag and lift forces around four different spoon shapes as they rotate through moving water. Each design had the same surface area, with different positions of maximum depth along their length. Experimental analyses used telemetry to measure blade forces during a series of rowing runs, for two different Concept2 blades, over different stroke rates and blade gearing. The results showed there was a correlation of R^2=0.78 between the location of the spoon's maximum depth and the lift force generated at the catch. The study also found that, a resultant fluid force change of 47.3 N, at the spoon, can promote a -10.7° ± 1.7° shift in the maximum force angle in the real world. The shift in maximum force angle highlighted how spoon design, especially regarding position of the maximum depth, affected the profile of the rowing stroke.

Keywords – oar, drive phase, fluid forces, lateral velocity, max force angle, power curve, gearing, computational fluid dynamics, concept2, rowing.

Definition of rowing terms

Gearing – The relationship between the inboard length and the overall length shown in Fig. 1
Catch – The point at which the spoon enters the water
Finish – The point at which the spoon leaves the water
Gate – A device that attaches the blade to the boat and allows it to pivot around a fixed point
Concept2 – Rowing equipment manufacturer
Collar – Circular ring attached to the shaft of the blade that can be adjusted to change the gearing of the blade. It also provides a point for the blade to rest up against the gate

1. INTRODUCTION

Rowing blades have been used for thousands of years, with designs remaining similar until the 1829 Oxford-Cambridge Boat Race sparked technological development, leading to 1-1.5% annual performance increases until rowing's 1900 Olympic debut [1-3]. During the 1900s, blades became up to 25% shorter, allowing crews to reach higher stroke rates [4]. The Macon blade (1958) introduced a shorter, wider spoon for better water connection. During the 1980s, composite materials allowed more complex, lighter blade designs [5].In 1991, Concept2 introduced the first asymmetrical cleaver blade, the Big Blade, which current spoon designs largely resemble [5]. Rowing blades (oars) consist of the handle, composite shaft, collar, and spoon, shown in Fig. 1. The spoon provides resistance for rowers to pivot the boat forward and their dimensions vary depending on the manufacturer and model. Rowing is typically contested over a 2000m course, requiring high forces over prolonged periods [6]. Fluid forces around the face of the spoon play a vital role, characterised by unsteady 3D flow with violent free surface deformation [7].

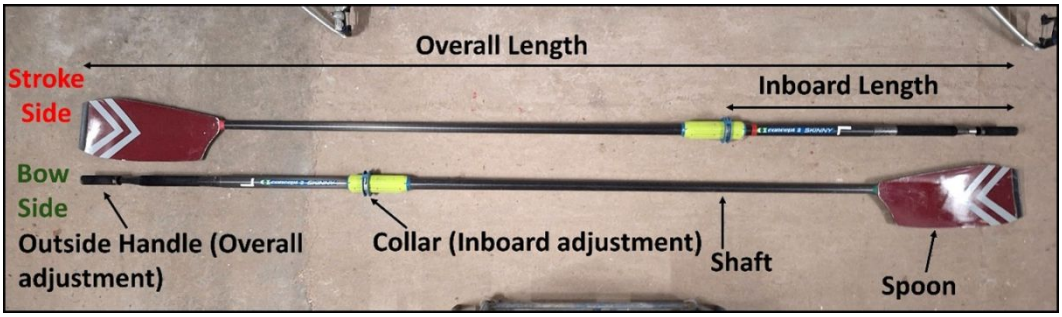

Figure 1. *Rowing Blade (Oar) Showing Key Features.*

With victory margins often within tenths of a second, efficient rowing equipment is crucial. The blade accounts for 21.7% of energy losses during the stroke compared to 1.1% for the boat [8]. This study aims to evaluate how different Concept2 spoon shapes influence power distribution and fluid forces throughout the stroke. Concept2 currently manufactures six different spoon designs, as seen in Table 1, each one with a unique load profile across the stroke [9].

Table 1*: Concept2 Spoon Designs [9].*

Spoon	Blade Length (mm)	Width at Tip (mm)	Width at Broadest Point (mm)
Comp	435	190	260
Fat2	550	190	265
Smoothie2 Vortex Edge	545	190	255
Smoothie2 Plain Edge	545	255	255
Big Blade	555/520	255	255
Macon	580/580	180/165	210/200

The rowing stroke comprises of two main phases, drive and recovery, with these phases attributing to 40% and 60% of the stroke respectively [4]. The speed of the stroke is important with stroke rates of 32-40 strokes per minute achieved during races, resulting in stroke cycle durations of 1.5-1.88 s [8]. The drive consists of multiple different sections, characterised by the angle of the gate and applied force (Fig. 2). During the drive, the blade remains fully submerged in the water with the top edge covered [10], 46.4% of the power comes from the rower's legs, 30.9% from the trunk, and 22.7% from the arms and shoulders [8].

The catch marks blade entry and drive phase start (Fig. 2a). For the first 5-15 degrees, pressure builds as the spoon loads. A resistive force threshold of 100 N must be overcome to accelerate the boat [11]. The slip angle extends from the catch to the point at which the 100 N threshold is overcome (Fig. 2a-b); the wash angle is from when force drops below 100 N to the finish (Fig. 2d). The finish occurs when the spoon exits the water, ending the drive phase [8] (Fig. 2e). The recovery aims to maintain boat momentum while positioning for the next stroke [8].

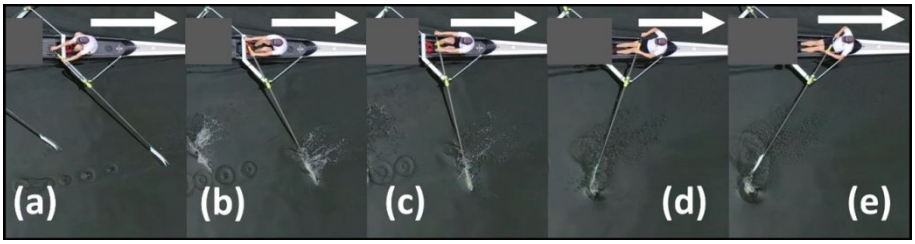

Figure 2. *A Visual Representation of the Key Points During the Drive: (a) The Catch, (b) Slip Angle, (c) Max Force Angle, (d) Wash Angle, and (e) The Finish.*

Due to the niche popularity of rowing, the amount of research carried out around blade design is limited, especially when compared to sports such as cycling which has a highly competitive sporting side and is a popular method of transport. This lack of research potentially limits the rate at which rowing could develop, highlighting the importance of researching the optimisation of the mechanical aspects of rowing and this study.

2. METHODOLOGY

During the drive phase, the relative motion of the spoon with respect to the water changes. The changes in blade angle cause the spoon to move away and towards the boat from the catch to the finish as shown in Fig. 2. Blade motion has previously been broken down into four sections by the founders of Concept2, shown in Fig. 3 [5]. This motion illustrates the two hydrodynamic forces that act on the blade during the drive cycle; drag force, F_D, and lift force, F_L, both of which depend on the design of the blade and its interaction with the water [12]. These forces cause a blade to behave in a similar way to an aerofoil due to the lateral motion of the blade and its curved surface [5]. The drag force is the dominant of the two forces during the drive and therefore contributes the most to boat velocity [1]. A major part of a blade's efficiency and success depends on its design and ability to generate the correct fluid forces during each phase of the stroke [5]. The Big Blade from Concept2 introduced a curved profile which showed an increased ability to generate fluid forces compared to the flat profile of the Macon that it descended from. However, it has been shown that although lift is dominant at the beginning and end of the stroke, a curved blade did not perform significantly better at angles of attack below 90° (between the max force angle and wash angle Fig. 2c and 2d) [12].

For all four phases of the stroke, the drag force, F_D, acts perpendicular to the lift force, F_L, with the net force, F_{Net}, being a sum of both vector forces. These forces act perpendicular to the blades chord line [1, 10], as shown in Fig. 3. During Phases 1 and 2, lift is the dominant force as the blade begins to accelerate through the water [4]. By Phase 3 the magnitude of the drag force increases as the lateral movement decreases, and the blade begins to move perpendicular to the hull of the boat [1]. The drag force therefore has the largest contribution to the forward motion of the boat [1]. At the end of the drive, by Phase 4, the forces are the same as Phase 2 but with the drag force in the opposite direction. The change in direction from Phases 1 and 2, to Phase 4 means that both the tip and shaft end of the spoon alternate in being the leading edge, making the rectangular spoon design optimal for equal lift in both directions [5].

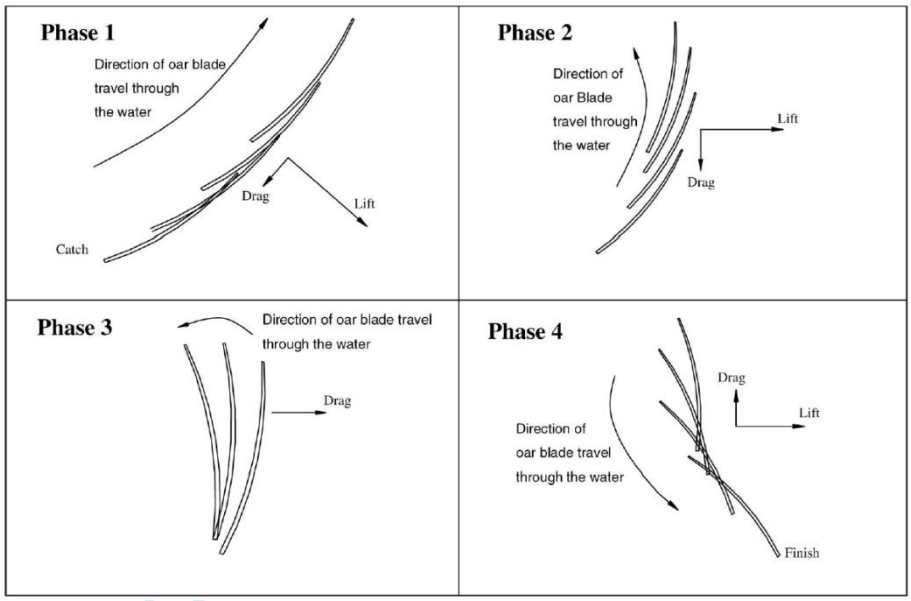

Figure 3. *The Four Phases of the Drive [5].*

2.1. Computational Methodology

Simulations were performed to investigate the comparative hydrodynamic behaviour of the candidate rowing blade geometries. The computational domain included the blade geometry immersed within a fluid domain representing the surrounding water. The mesh was generated using an unstructured grid with local refinement applied in the vicinity of the blade surface to capture pressure gradients around the leading and trailing edges.

The governing equations were solved using the finite volume method implemented in ANSYS Fluent. Turbulence effects were represented using an SST k–ω turbulence model. Pressure–velocity coupling and second-order spatial discretisation schemes were used to improve numerical stability and solution accuracy for the momentum and turbulence transport equations.

2.2. Computational Setup

A quasi-static approach was used where fluid flow was analysed at different blade angles to predict how the lift and drag of the spoon varies as it rotates around 360°. A typical rowing arc is ~90°, however, to accurately capture the full fluid behaviour around the spoon a much larger angle range needed to be tested. During Phase 1 the fluid velocity is flowing over the tip of the spoon ± 15°. During Phase 2 the spoon starts to reach the peak of the arc and the angle of the fluid starts to change towards the face of the spoon. During Phase 3 the fluid velocity is now almost fully on the face of the blade. When the spoon reaches Phase 4 the fluid velocity is now in the opposite direction to Phase 1 and is on the shaft end of the spoon ± 15°. The large angle range of fluid forces experienced during the drive led to a full rotation being simulated to ensure that the full fluid behaviour is captured and no data was lost. Similar quasi-static approaches have been previously used when modelling kayaking and swimming [13]. Assuming a constant angular velocity throughout the stroke cycle and that the drive phase takes up 40% of the stroke cycle [4], the lateral velocity, v, of the spoon in relation to the boat can be calculated using:

$$v = \frac{x_{out} - (x_{out} \cdot sin(90 - \alpha_{catch}))}{\left(\frac{\left(\frac{60}{\beta} \cdot 0.4\right)}{\alpha_{total}}\right)\alpha_{catch}} \quad (1)$$

where, β is the rate in stroke per minute (spm), x_{out} is the outboard length (collar to blade tip) and α relates to the gate angle. Using Equation 1, with stroke rate, β, of 36 spm, an outboard length, x_{out}, of 255.5 cm, α_{catch} of 55° and α_{total} of 90°, the velocity was calculated to be 2.55 m/s.

To evaluate the effect of spoon shape on lift and drag forces during the stroke, four different spoon shapes were analysed using 3D CFD. Each of these designs, shown in Fig. 4a, had equivalent front face areas of 1196.27cm² ± 0.00065 cm² to prevent area from influencing the drag and lift forces. The spoons were made up of seven sketches that were lofted together, allowing for the easy adjustment of dimensions to create all four spoon designs Fig. 4b. Design 1 was the 1:1 scale replica of a Smoothie2 blade, Design 2 took inspiration from the Fat2 spoon with a maximum depth of 265mm on sketch plane 2 of 7. Designs 3 and 4 kept the same maximum depth of 265mm, however the maximum depth was moved towards the shaft to understand how location has an effect on the fluid forces, sketch plane 4 of 7 in Design 3, sketch plane 5 of 7 in Design 4. All four designs had a shaft attached to the spoon, the shaft was of uniform diameter of 45mm and was 1000mm long so the end would leave the fluid domain. The shaft dimensions were the same for all spoons preventing this from affecting the results. The SolidWorks designs could then be exported as a Parasolid file into Ansys' Design Modeler.

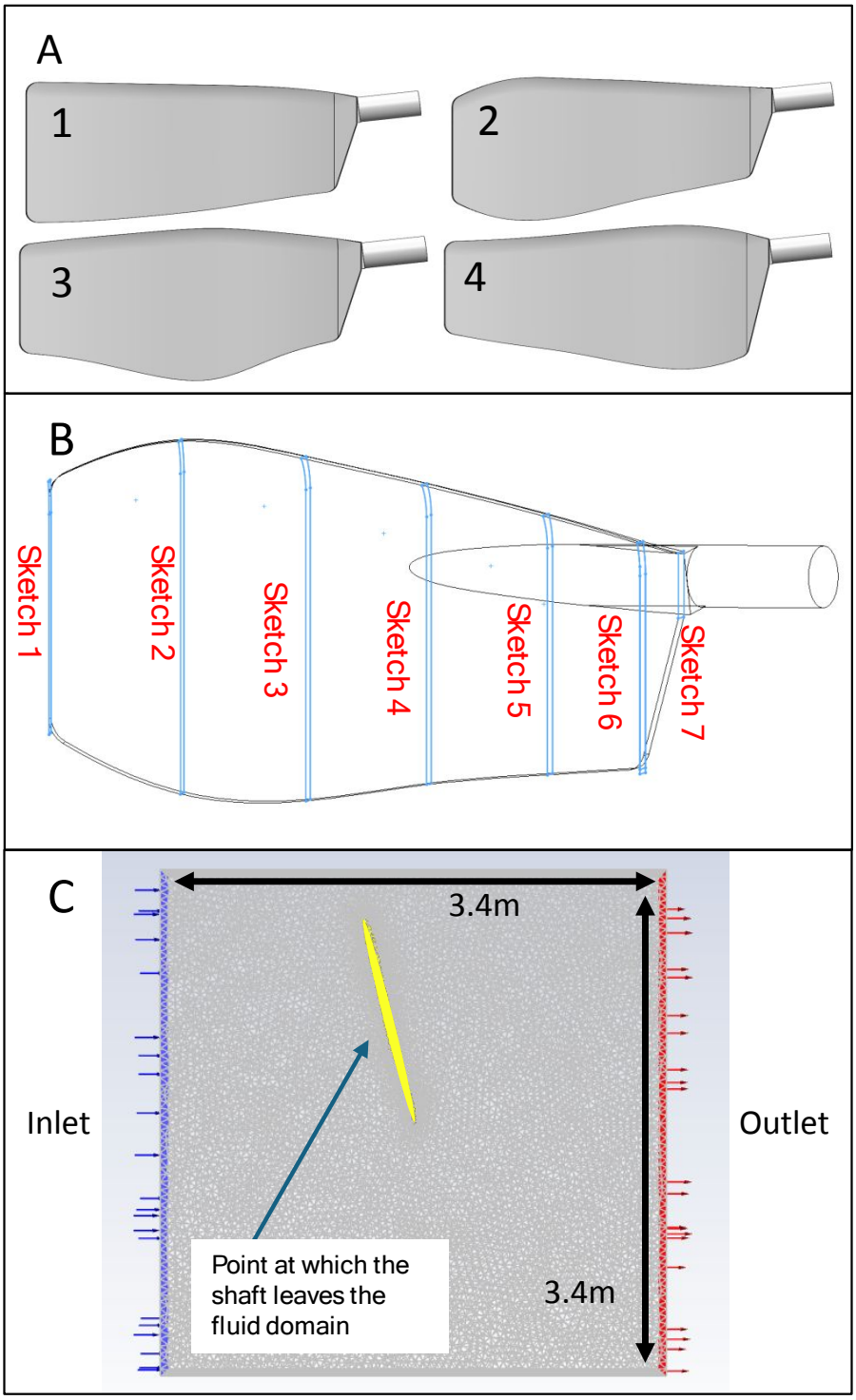

Figure 4. *(a) The Four Spoon Designs Used for the Study, (b) SolidWorks Profile of Smoothie2 Spoon Showing Sketch Planes 1-7, (c) Boundary conditions for the 3D model showing the point at which the shaft leaves the fluid domain.*

A Boolean subtraction tool used for the fluid domain for each of the four test blades. For the study, a cube shaped domain of edge length 3.4 m was used, the boundary conditions for this set up can be seen in Fig. 4c. The 3D study allowed for different spoon depths to be tested. A body transformation rotate tool was used to allow for multiple angles of attack to be simulated. The process of setting up the study involved testing all four designs at each angle of attack (AOA), using Ansys

Fluent. The parameter set was used to calculate the drag force/coefficient and the lift force/coefficient every five degrees for each blade design resulting in 1152 data points being calculated.

The parameters used to set up the CFD study can be seen in Table 2, which used: Ansys DesignModeler for the geometry, Ansys Meshing for the mesh and section naming, Ansys Fluent for the boundary conditions and simulations, and Ansys Fluent CFD post for the contour plots. The data could then be exported via a CSV file from the parameter set on Ansys Workbench.

Table 2. *Parameters used for 3D CFD Model*

DesignModeler Settings:	
Fluid Domain (m)	±1.70,0.29/-0.20, ±1.70
Rotation Y Axis (m)	-0.05, -0.05
Mesh Settings:	
Element Size	50
Max Size (mm)	50
Inflation	N/A
Defeature Size (mm)	0.25
Curvature Min Size (mm)	0.5
Maximum Layers	N/A
Growth Rate	N/A
Fluent Settings:	
Model	SST K-ω
Fluid	Water-Liquid
Inlet Velocity (m/s)	2.255
Reference Length (m)	N/A
Force Vector Lift	X (-1), Y(0), Z(0)
Force Vector Drag	X (0), Y(0), Z(-1)

2.3. Experimental Procedure

To validate the computational models used, an experiment was carried out using equipment provided by Swansea University Rowing Club. The experiment involved a coxed four (four-person crew with coxswain) completing six test runs with different blade designs and set ups. The experiment was performed over two days on the River Tawe, both days with similar atmospheric conditions. During the experiment the cox's instructions were limited to the timing of the rate changes only, this was to provide consistency between test runs.

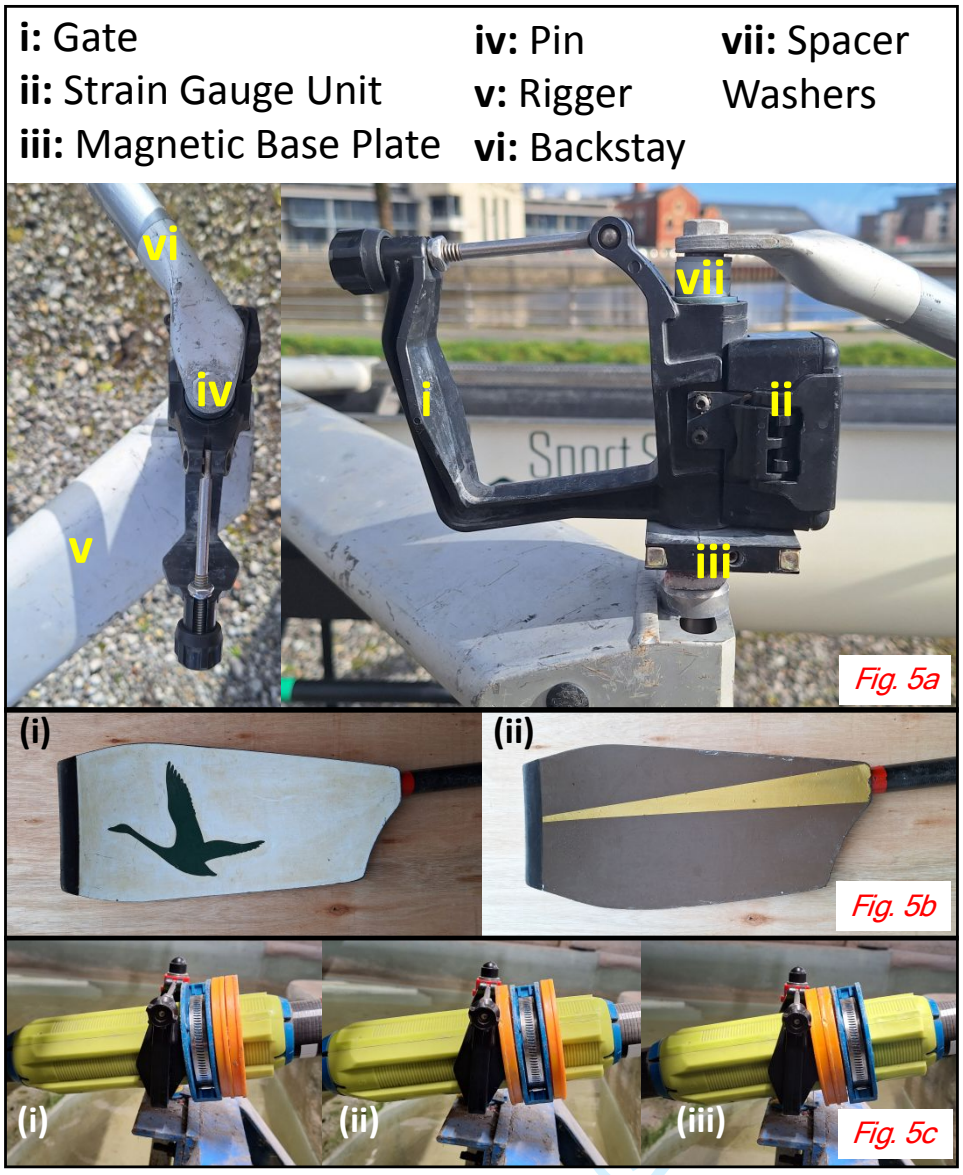

Figure 5. Fig. 5a: NK Empower-Oarlock Telemetry, *Fig. 5b: (i) Smoothie2 Vortex edge, (ii) Fat2, Fig. 5c: Clam Adjustment for the Experiment, Spoon to the Left of the Image and Handle to the Right, (i) Inboard 114.5cm, (ii) Inboard 115.5cm (iii) Inboard 116.6cm*

2.3.1. Telemetry

To record data on each test run, rowing telemetry was used. Each seat in the boat had its own telemetry gate allowing four sets of data to be gathered during each test run. The telemetry gates used were NK empower-oarlock gates (Fig. 5a) paired with the NK SpeedCoach GPS. The SpeedCoaches were set up so the rowers could not monitor their power outputs, preventing self-adjustment and potential bias. For each stroke taken, multiple data points were recorded and subsequently downloaded as a CSV file post experiment.

All rowers used for this experiment were members of the Swansea University Rowing club and had a minimum of 3 years experience in the sport. Prior to the experiment taking place an ethics form was completed in accordance with the University's guidelines. The ethics form included consent from all of the athletes taking part.

2.3.2. Blades Used

Two different spoon types were used in this test, both manufactured by Concept 2: the Smoothie2 Vortex Edge and the Fat2, Fig. 5b. These spoons were chosen to validate the computational data from Designs 1 and 2. The gearing was set on all eight blades to 370cm overall and 114.5cm inboard. Both the blades used Concept 2's Ultralight shaft with a medium stiffness.

2.3.3. Test Runs

The overall length of the blade was not changed to reduce the number of test runs, the inboard was adjusted during the experiment by the rowers. A clam, was added to increase the inboard after each test run (Fig. 5c). This process was done twice per blade, resulting in six test runs, seen in Table 3. Each test run was carried out over five minutes; the first two minutes were done at 20 strokes per minute, which is a typical paddling rate used during training sessions. The rate then increased every minute to 24, 26, and 28 strokes per minute. The five-minute data collection period began once the boat was up to speed, and the rate had settled at 20 strokes per minute, resulting in 24 tests overall.

Table 3: *P*arameters for experimental test runs

Test Run	*Test Numbers*	*Overall (cm)*	*Inboard (cm)*	*Spoon Shape*	*Shaft Design*	*Rate*
1	1-4	375.0	114.5	Fat 2	Ultralight	20-28
2	5-8	375.0	115.5	Fat 2	Ultralight	20-28
3	9-12	375.0	116.5	Fat 2	Ultralight	20-28
4	13-16	375.0	114.5	Smoothie2	Ultralight	20-28
5	17-20	375.0	115.5	Smoothie2	Ultralight	20-28
6	21-24	375.0	116.5	Smoothie2	Ultralight	20-28

3. RESULTS

3.1. Computational Results

The 3D simulations were used to evaluate the flow behaviour around four different spoon shapes, obtaining drag and lift forces as the spoons rotate around 360° with respect to fluid flow. Fig. 6 shows that all four designs produce a similar peak drag force of ~600 N at 14° and ~500 N at 200°. The drag force continued to show similar behaviour for all spoon designs for the majority of the cycle apart from between 75° - 100° and 300° - 320° where the B1 decreased first followed by B2, B3 and B4.

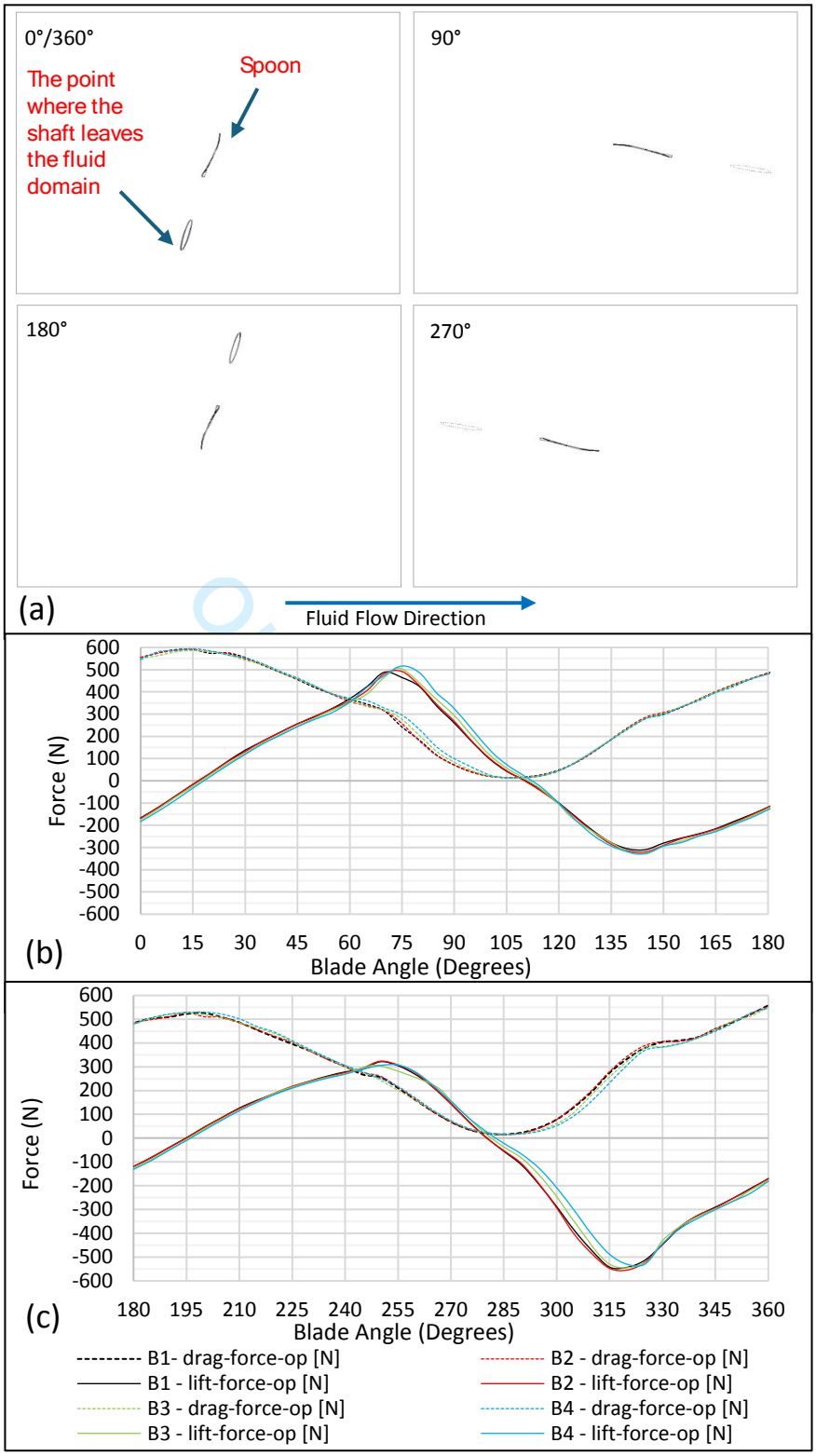

Figure 6. *Predicted Drag and Lift Forces for all four Spoon Designs: (a) Blade Rotation Diagram with the Spoon in the Centre of the Fluid Domain and Point at which the Handle Leaves the Fluid Towards the Outside., (b) Forces 0° - 180°, (c) Forces 180° - 360°.*

3.2. Experimental Results

The force curves were taken from the average forces across all rates for each gearing, comparing both the spoon shapes. Fig. 7 shows that for the front oarsman's data (stroke seat), the Fat2 spoon

promoted an average peak force increase of 131.3 N ± 26.3 N, this caused an average power increase of 27.5% (area under the curve).

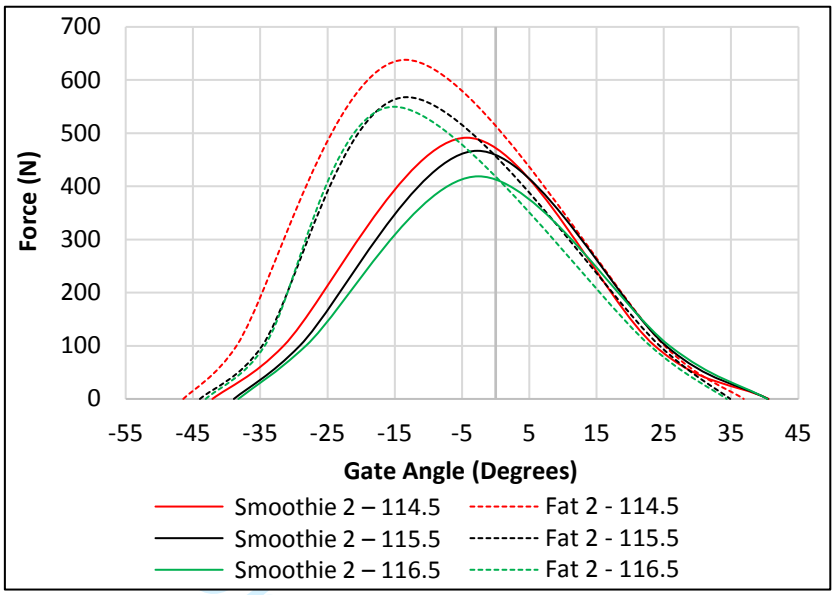

Figure 7. *The Average Power Curve Data for all Rates of the Stroke Seat for Both Blade Types at Each Gearing.*

The influence the spoon design has on the characteristics of the stroke, (Fig. 8 and 9), for all 24 tests. The data showed that as the inboard length increased, the catch angle decreased and that the maximum force angle, at each gearing, was earlier on in the stroke with the Fat2 by -10.7° ± 1.7°.

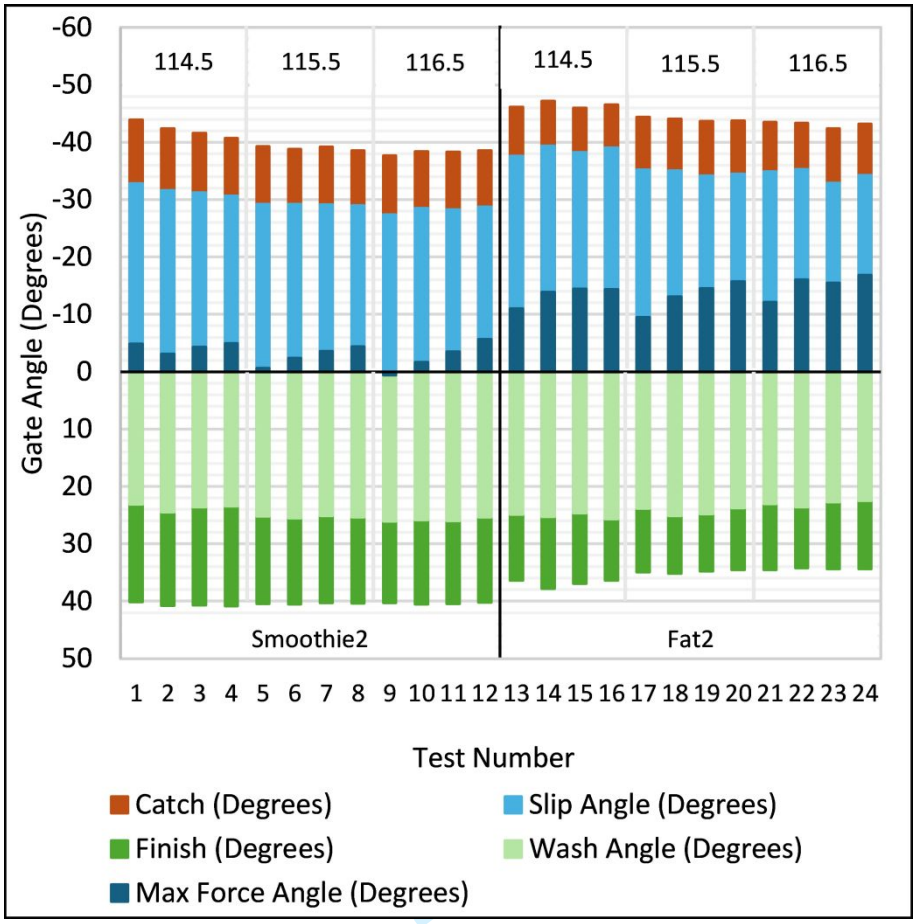

Figure 8. *The Average Gate Angles at Each Key Stroke Markers for all 24 Test Runs.*

The measured force at the gate, F_{gate}, can be related to the applied force at the handle, F_{hand} using [8]:

$$F_{hand} = F_{gate} \frac{L_{in-a}}{L_{in-a} + L_{out-a}} \quad (2)$$

where L_{in-a} and L_{out-a} are the blades gearing values seen in Table 3 and F_{gate} is obtained from telemetry force values. Using Equation 2, the maximum and average handle forces are calculated across all 24 tests, shown in Fig. 9. This figure shows that there is an increase in both force and power as stroke rate increases. Also, as the gearing increased there was a decrease in power and force for both the Smoothie2 and Fat2 blades. This data shows a strong correlation between max force and power throughout the stroke. A clear difference between the force and power obtained for each spoon, the Smoothie2 and Fat2, is visible for all gearing and stroke rates tests. The percentage differences for all measured variables between the two spoons are shown in Table 4.

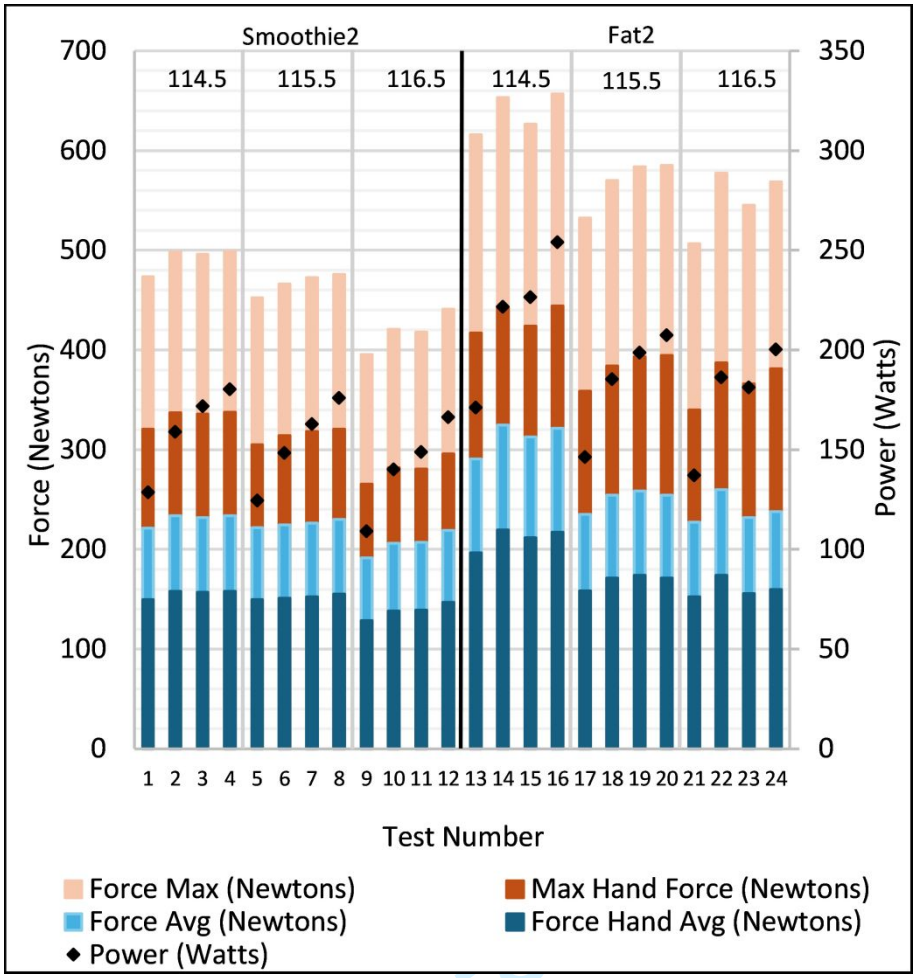

Figure 9. *Comparison of the Force and Power Across all 24 Tests.*

Table 4. Percentage Change for all Variables from Smoothie2 to the Fat2

Gearing	*114.5*	*115.5*	*116.5*
Power	36.3	20.6	25.1
Catch	10.3	12.9	12.7
Slip	-25.2	-5.5	-12.5
Finish	-9.2	-13.8	-14.9
Wash	-30.5	-30.6	-21.7
Force Avg.	35.7	11.0	16.3
Work	38.3	22.1	27.4
Force Max	29.8	21.6	31.2
Max Force Angle	225.5	628.4	-168.4
Total Length	0.7	-0.7	-1.5
Effective Length	15.3	8.5	6.0
Speed (GPS)	9.0	9.6	2.5
Distance/Stroke	11.5	12.7	3.4
Ra-m	4.6	-8.8	-11.4

This comparison was done using the average of all the rates at all the three tested gearings. The total length was calculated using Equation 3 [8]. The R_{a-m} was calculated using Equation 4 [8], this gives an indication of the curve smoothness with smoother curves suggesting a reduction in stroke velocity fluctuations [14].

$$\alpha_{total} = \alpha_{finish} - \alpha_{catch} \quad (3)$$

$$R_{a-m} = \frac{F_{avg}}{F_{Max}} \quad (4)$$

where F_{avg} is the average force during the drive phase and F_{Max} is the maximum force during the drive phase. The change in gearing affected the arc of the blade as it moves through the stroke (Fig. 10). The increased inboard makes it harder for rowers to reach the front of the stroke therefore reducing the catch angle. The reduced catch angle results in a total length reduction of 5.0% (4.1°) with the Smoothie2, and a 7.0% (5.9°) decrease with the Fat2. The reduced catch angle leads to a smaller arc meaning that the effective stroke length when the boat is being accelerated also decreased by 2.2% (1.2°) with the Smoothie2 and 10.0% (6.4°) with the Fat2.

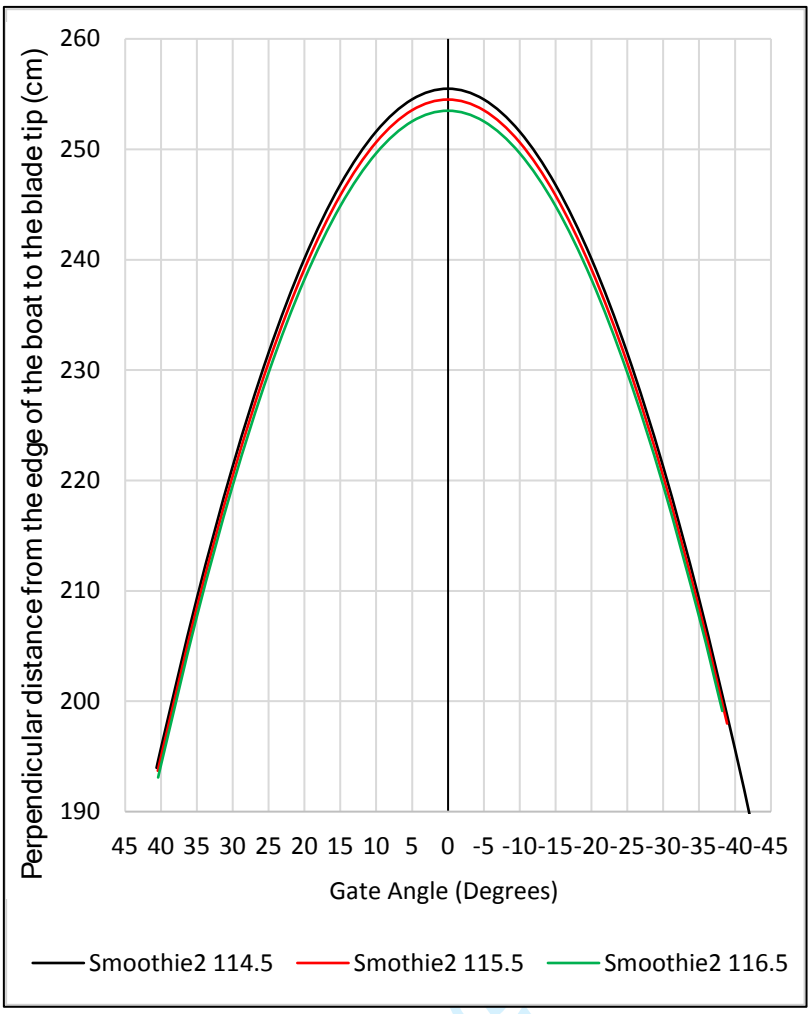

Figure 10. *Change in the Middle of the Arc profile with Gearing.*

The speed and distance per stroke of all 24 tests compared to the recorded power output (Fig. 11). The parameters measured in the experiment were averaged across all rates to reduce the effect of the environmental conditions on the results. For all tests the power output was higher with the Fat2 than the Smoothie2, with an average increase of 27.3% (41.6 W).

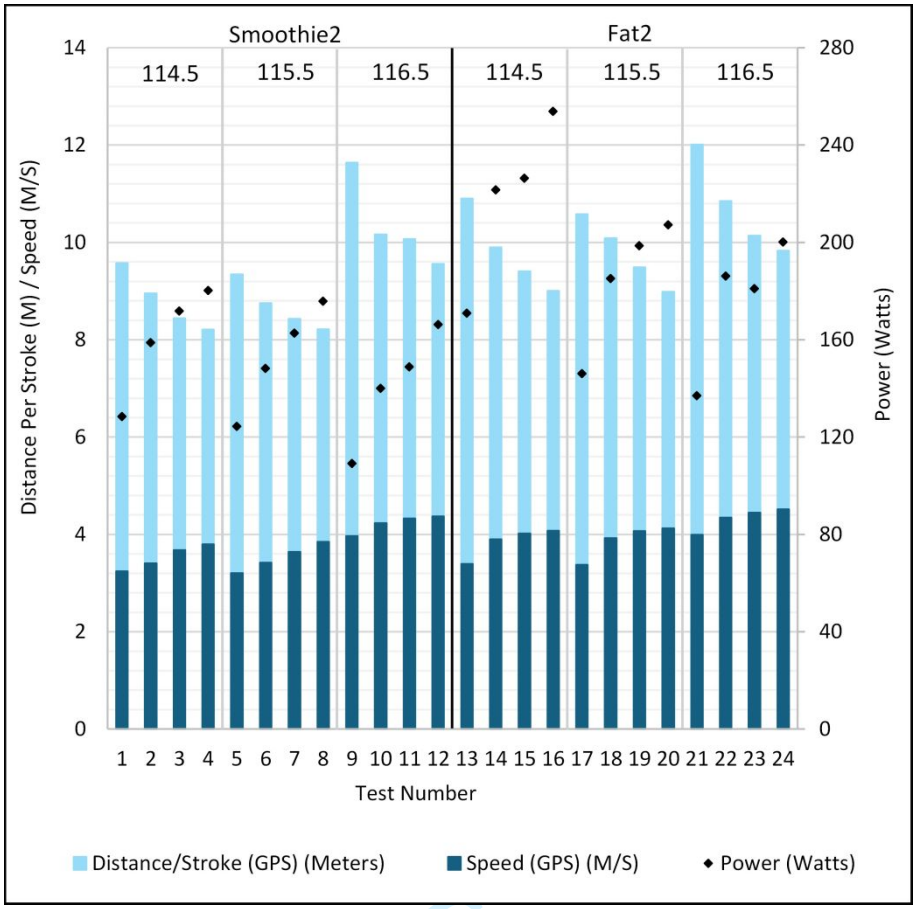

Figure 11. *Comparison of Power and Speed Across all 24 Tests.*

The rate behaved similarly for both blade designs with a peak force earlier on in the drive phase as the rate increased as the rowers tried to maintain a higher boat speed. There was greater change with the Fat2 with a 6.0° change in peak force between 20 SPM and 28 SPM compared to the Smoothie2's 3.8° change (Fig. 12).

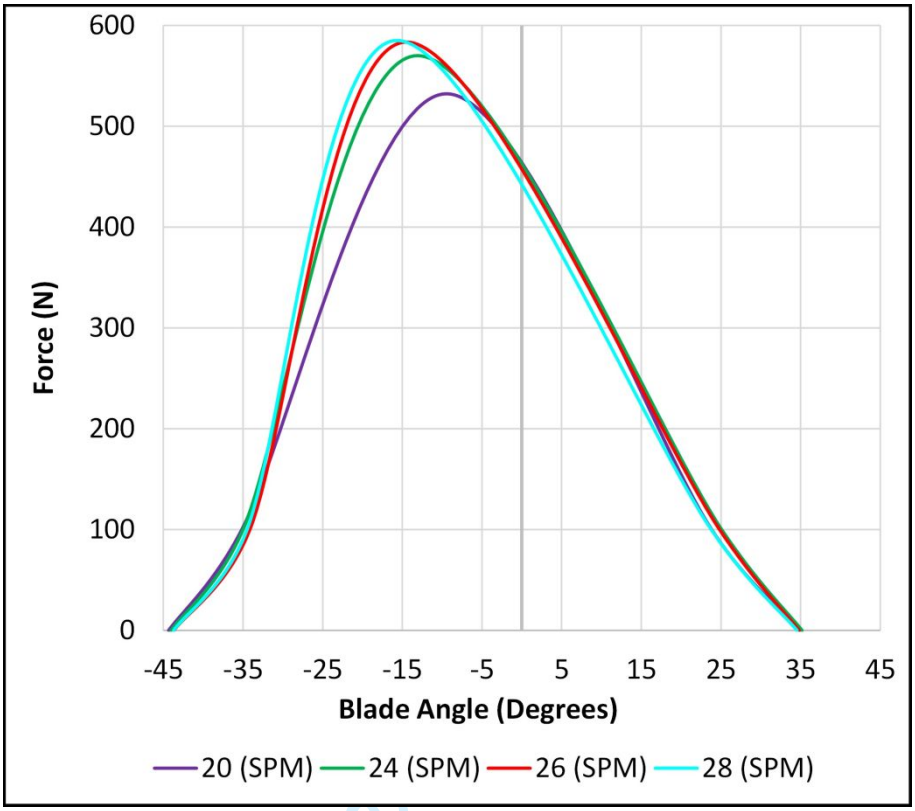

Figure 12. *The Effect of Rate on the Distribution of Power on the Fat2 Spoon, 115.5cm Inboard.*

4. DISCUSSION

The propulsive efficiency of a spoon through the drive phase depends on the ratio of the blade forces (lift and drag) compared to the blade area. During the four phases of the drive a combination of drag and lift forces exist around the spoon (Fig. 3). The face of the spoon builds up a large resistive force against the body of water that it is in contact with. Resistive forces form a pocket of water around the face of the spoon which provides a point of leverage that works in tandem with the pivot point of the gate to propel the boat forward. However, the path of the blade is more complex, and the spoon moves perpendicular to the boat as the blade pivots in the gate. This motion, first observed by Kleshnev [15], can be tracked throughout the stroke cycle as the boat moves past the pocket of water, shown in Fig. 13. The lateral motion is due to the arc that the blade makes as it pivots around the pin of the gate, where the maximum distance of the blade tip from the boat is when the blade is at 0° and perpendicular to the hull. The greatest lateral velocity occurs during the first two phases of the stroke as the blade approaches perpendicular during the leg drive. During the drive, 60° to 45° of blade movement takes place before perpendicular, and 25° to 35° takes place after perpendicular, this leads to an asymmetrical elliptical blade path.

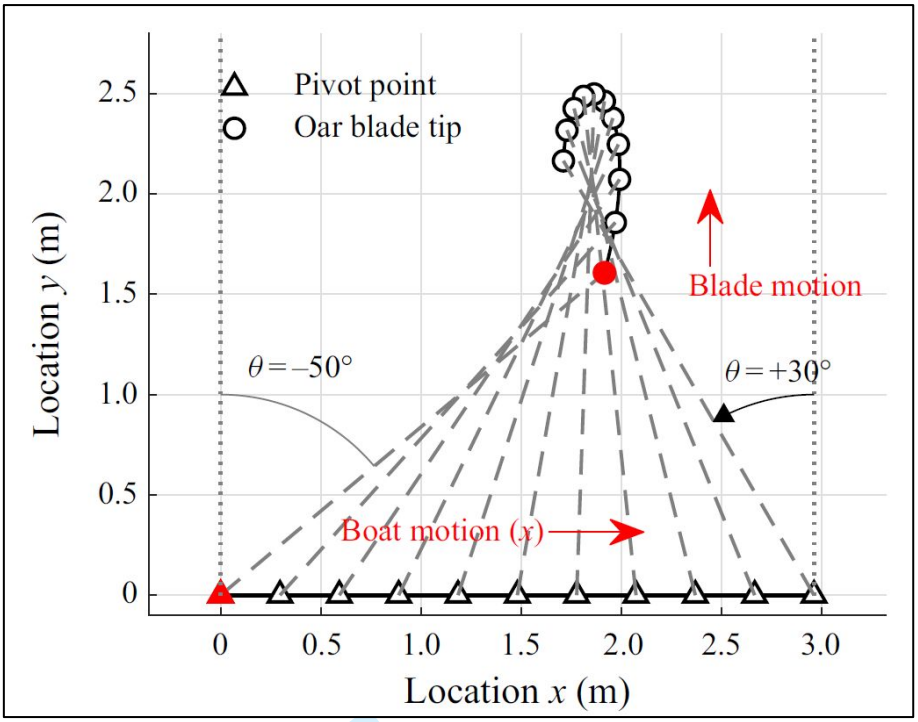

Figure 13. *A Generic Blade Path Compared to Boat Motion [16].*

4.1. The Influence of Spoon Design

The 3D CFD study, showed that the maximum drag forces of different spoon shapes were similar, for spoons with the same surface area (Fig. 6). This maximum drag force occurred when the spoon was perpendicular to the water flow (Phase 3). However, the variation of lift for each spoon design varies as the angle of attack varies indicating that the spoon profile has a stronger influence on lift (Fig. 13).

All four spoon designs produced different fluid forces as the blade rotated through a full 360° cycle. Design 1 acted as the control, Designs 2-4 showed the effect that the location of the greatest depth had on the fluid forces. At the catch angle, Design 2 produces the greatest drag out of all the designs due to its increased profile around the tip, this will provide a greater resistive force for the rower to leaver from. By reducing the amount of wasted energy around the catch, there is an increased power reading and greater boat acceleration. For the lift force, the greatest lift (Phase 2) occurred at ~70°. Design 4 produced the highest simulated lift, which dropped across Designs 3 and 2 by 4.7%. For the highest negative lift at ~320° (Phase 4) the order was reversed with Designs 2, 3, and 4 respectively experiencing a comparative drop of 4.5%. The drag displayed similar trends between 75° -100° where Design 4 produced the highest drag and Design 2 produced the lowest. Between 295° -325°, Design 2 produced the highest drag and Design 4 produced the lowest. Between 295°-325°, Design 2 produced the highest drag and Design 4 produced the lowest. For both angle ranges, Design 3 produced a drag force between Designs 2 and 4. The profiles of Designs 2 and 4 show large resemblance to that of a Delta wing, with both edges becoming the leading edge during the drive phase. Both Designs 2 and 4 showed opposite fluid force behaviour during testing. For Design 2 (during Phase 4) and Design 4 (during Phase 1) the distance between the two edges increases from leading edge to trailing edge. It is possible that larger vortices could have developed around both edges, causing the fluid flow to remain attached to a greater portion of the back surface, which would result in greater lift [5]. The effect of vortices on the fluid forces around the spoon could be further investigated in a future study.

4.2. Experimental validation

The experimental data gathered shows a significant change in stroke characteristics and power distribution between spoon designs (Figs. 7-9). The Fat2 design promoted peak power earlier on in the drive phase, this was validated with a 3D study when comparing Designs 1 and 2. Design 1 was a replica of the Smoothie2 with a much more rectangular profile and Design 2 took inspiration from the Fat2 with a deeper profile towards the tip of the blade. Design 2 showed a greater spoon drag force around the catch angle (45° experimental, 315° ± 10° computational) with a 2.4% ± 0.9% (5.5 N ± 0.7 N) increase. The increase in drag force at the spoon that led to an increase of 12.4 N ± 1.4 N at the handle and 19.0 N ± 2.1 N at the gate. At the point where the blade travels laterally from Phases 1 to 2 (90° ± 10° computational) there was a 2.7% ± 0.5% increase (7.8 N ± 0.2 N) in lift force in Design 2. The increase in lift led to a 20.6 N ± 4.8 N force increase at the handle and 30.5 N ± 7.1 N at the gate. During Phase 1 for Design 2, the resultant magnitude of the fluid forces were 47.3 N higher. The increase in fluid forces during the beginning of the drive, as shown with the Fluent data (Fig. 6), explains the change in the max force angle for the Fat2 by -10.7° ± 1.7°. It has been shown that the parameters, mean and peak force have the greatest effect on velocity, without power adjustment, for all boat classes, showing a strong relationship between peak force and velocity [14]. The change in force observed in the computational study was lower than that observed in the experiment. The promoted max force caused by the shape of the spoon is -10.7° ± 1.7° earlier in the drive, this allows a greater engagement from the abductive quadricep muscles, accounting for 46.2% of power during the drive [8]. The proxy mechanical power calculated using rowing telemetry tends to be 10% greater than the true mechanical power outputted by the rower [17]. Design 2 was not a 1:1 scale replica of a Fat2, although it did have the same width at the tip, maximum depth, and length. The difference between Design 2 and the Fat2 are as followed; sketch 1 (0mm), sketch 2 (+5mm), sketch 3 (-4mm), sketch 4 (-16mm), sketch 5 (-20mm). sketch 6 (-15mm), sketch 7 (+3). These factors explain the discrepancy between the experimental and computational data.

The spoon's maximum depth position (Planes 1-7) allows for peak force adjustment, with R^2=0.78 between the maximum depth location and the catch lift force. Therefore, relating back to the location of the peak power during the drive, as shown by the comparison of the computational results and telemetry data. Rowing technique has typically evolved from a trial-and-error approach alongside adopting the style of winning crews [18]. This research has allowed for an analytical approach for crews and coaches to optimise their performance by tailoring a spoon design to their specific style. This could be applied at all levels of the sport from an amateur club right up to Olympic athletes.

4.3. Fluid Velocity

For this study the lateral velocity was chosen to be 2.55m/s using a stroke rate of 36 spm, an outboard of 255.5 cm and assuming a total length of 90°. As the spoon of a blade behaves in a similar way to an aerofoil there are three main parameters that affect the stall angle and lift forces; angle of attack, profile and fluid velocity [19]. During this study the spoon profile and AOA have been investigated and how these factors affects the corresponding fluid forces around the face of the spoon. The velocity however has been consistent throughout. Using Equation 1 the effect of gearing rate on the average lateral velocity can be seen on Fig. 14. The difference in gearing and rate between an amateur crew and high-end athletes could lead to the lateral velocity being double for the top end crews. Further research at different velocities would then allow for blade allocation depending on the expected calculated lateral velocity of a crew.

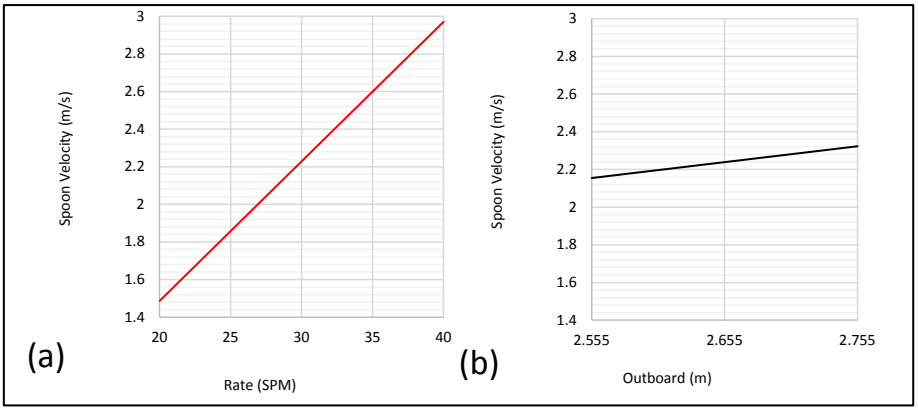

Figure 14. *Relationship Between SPM (at an out board of 255.5cm)/Outboard and Spoon Tip Velocity.*

Muscular efficiency of any athlete is limited, leading to a compromise of blade area [3]. Efficiency is also highly linked to the speed and type of boat used, with higher efficiency in faster moving larger boat classes. There is a mechanical increase in blade efficiency from 78.5% in a single manned boat to 85.3% in an eight manned boat [15]. This study shows that spoon profile, in particular the position of the spoon's maximum depth, influences the distribution of lift and drag forces during the rowing stroke. This, in turn effects the power curve during the full stroke.

4.4. Computational Lateral Velocity Limitations

For the purpose of this study the lateral velocity of the tip of the blade is assumed to be constant throughout the stroke cycle. This motion differs from the real-life motion of the blade. During Phases 1 and 4, the spoon tip will experience a much higher velocity compared to Phases 2 and 3 (Fig. 3). This acceleration and deceleration would alter the lift and drag forces throughout the drive. If a future study was carried out where the velocity changed during the drive this could add greater depth and understanding to the results gathered.

The lateral velocity was decided using Equation 1 at a stroke rate of 36 spm, a typical race rate for high level crews. This differs from the rate used during the experimental testing (20 – 28 spm), to try and prevent muscular fatigue from affecting the results of the data, the experimental rates were kept lower. The computational rate needs to be higher to amplify the drag and lift forces making comparison easier, causing some discrepancy between the experimental and computational results.

4.5. Near-Wall Treatment Limitation

A limitation of the present numerical study is that the CFD model does not explicitly resolve the boundary layer due to the absence of inflation layers in the mesh. Additionally, a formal mesh-independence study was not undertaken. These factors introduce uncertainty in the absolute magnitude of predicted hydrodynamic forces. However, the CFD model was applied consistently across all blade geometries and therefore remains useful for identifying relative trends in blade performance within the scope of the design study.

5. CONCLUSIONS

This paper presents a combination of computational modelling and experimental work to explore the effects of spoon shape on rowing performance. A 3D CFD study has shown that lift and drag vary as the spoon rotates with lift peaks occurring at blade angle of 74° and 250°. The peak drag corresponds to the spoon angle at max force and peak lift corresponds to an angle early in Phase 1 of the stroke. A spoon with greatest depth towards the blade tip (Design 2) exhibits the lowest drag and

lift forces during Phase 1 of the drive. A spoon with the greatest depth towards the blade shaft (Design 4) displays the highest forces during this phase.

An experiment comparing the rowing behaviour of two different spoon designs, showed that the spoon with the greatest depth (Fat2) had an earlier and greater peak force than the Smoothie2 spoon. This is due to the greater contribution of fluid forces during the early part of the drive (Phase 1). This observation correlates well with the behaviour predicted by the CFD model. A higher stroke rate produces an earlier peak in force. This is due to a combination of greater resistive forces, but also a greater spoon velocity perpendicular to the boat motion, increasing the lift force during Phase 1. This research provides a greater understanding of the role of spoon shape throughout the full drive phase of a rowing stroke, aiding the designers in producing spoons that align to the performance of individual rowers and configurations of boats.

6. Acknowledgments

The Authors would like to thank Swansea University Rowing Club for allowing the use of their equipment, and the five athletes (four rowers, one cox) who took part in the study. Thank you to Monmouth School Rowing Club who provided the Fat2 blades for the experiment.

7. References

[1] Fundel S. Development of a smart rowing blade (Doctoral dissertation, University of Applied Sciences Technikum Wien).

[2] Wigglesworth N. The social history of English rowing. Routledge; 2013 Oct 31.

[3] Kleshnev V. Rowing Biomechanics; 2006.

[4] Labbé R, Boucher JP, Clanet C, Benzaquen M. Physics of rowing oars. New Journal of Physics. 2019 Sep 24;21(9):093050.

[5] Caplan N, Gardner TN. A fluid dynamic investigation of the Big Blade and Macon oar blade designs in rowing propulsion. Journal of sports sciences. 2007 Apr 1;25(6):643-50.

[6] Almeida-Neto PF, Silva LF, Matos DG, Jeffreys I, Cesario TD, Neto RB, Barbosa WD, Aidar FJ, Dantas PM, Cabral BG. Equation for analyzing the peak power in aquatic environment: An alternative for olympic rowing athletes. PLoS One. 2020 Dec 17;15(12):e0243157.

[7] Robert Y, Leroyer A, Barré S, Rongère F, Queutey P, Visonneau M. Fluid mechanics in rowing: the case of the flow around the blades. Procedia Engineering. 2014 Jan 1;72:744-9.

[8] Kleshnev V. Biomechanics of Rowing. 2016 Jun.

[9] Cheri. Blades Overview and Loading Profile [Internet]. Concept2. 2012 [cited 2025 Mar 02].

[10] Sliasas A, Tullis S. The dynamic flow behaviour of an oar blade in motion using a hydrodynamics-based shell-velocity-coupled model of a rowing stroke. Proceedings of the Institution of Mechanical Engineers, Part P: Journal of Sports Engineering and Technology. 2010 Mar 1;224(1):9-24.

[11] GER VN. Introduction to the Biomechanics of Rowing.

[12] Caplan N, Gardner TN. Optimization of oar blade design for improved performance in rowing. Journal of sports sciences. 2007 Nov 1;25(13):1471-8.

[13] Lauder MA. Motion analysis in water sports. WIT Transactions on State-of-the-art in Science and Engineering. 2008 Apr 25;32.

[14] Holt AC, Aughey RJ, Ball K, Hopkins WG, Siegel R. Technical determinants of on-water rowing performance. Frontiers in sports and active living. 2020 Dec 3;2:589013.

[15] Kleshnev V. Propulsive efficiency of rowing. InISBS-Conference Proceedings Archive 1999.

[16] Grift EJ, Tummers MJ, Westerweel J. Hydrodynamics of rowing propulsion. Journal of Fluid Mechanics. 2021 Jul;918:A29.

[17] Hofmijster MJ, Lintmeijer LL, Beek PJ, van Soest AK. Mechanical power output in rowing should not be determined from oar forces and oar motion alone. Journal of sports sciences. 2018 Sep 17;36(18):2147-53.

[18] Sanderson BR, Martindale W. Towards optimizing rowing technique. Medicine and science in sports and exercise. 1986 Aug 1;18(4):454-68.

[19] Gu Z, Wang G. Effect of Reynolds Number and Angle of Attack on Aerodynamic Performance of NACA2412. Applied and Computational Engineering . 2025 Jan 13;130.